Induction of mismatch repair deficiency, compromised DNA damage signaling and compound hypermutagenesis by a dietary mutagen in a cell-based model for Lynch syndrome

IJsselsteijn, R.; Hees, S. van; Drost, M.; Jansen, J.G.; Wind, N. de

Carcinogenesis, 2022, **43**, 160–169
https://doi.org/10.1093/carcin/bgab108
Advance access publication 17 December 2021
Original Article

Induction of mismatch repair deficiency, compromised DNA damage signaling and compound hypermutagenesis by a dietary mutagen in a cell-based model for Lynch syndrome

Robbert Ijsselsteijn, Sandrine van Hees, Mark Drost[1], Jacob G. Jansen* and Niels de Wind*

Department of Human Genetics, Leiden University Medical Center, Leiden, The Netherlands
[1]Present address: Department of Clinical Genetics, Erasmus Medical Center, Rotterdam, The Netherlands

*To whom correspondence should be addressed. Tel: +31 715269627; Fax: +31715268284; Email: J.G.Jansen@lumc.nl
Correspondence may also be addressed to Niels de Wind. Tel: +31715269627; Fax: +31715268284; Email: N.de_Wind@lumc.nl

Abstract

The prevalent cancer predisposition Lynch syndrome (LS, OMIM #120435) is caused by an inherited heterozygous defect in any of the four core DNA mismatch repair (MMR) genes *MSH2*, *MSH6*, *MLH1* or *PMS2*. MMR repairs errors by the replicative DNA polymerases in all proliferating tissues. Its deficiency, following somatic loss of the wild-type copy, results in a spontaneous mutator phenotype that underlies the rapid development of, predominantly, colorectal cancer (CRC) in LS. Here, we have addressed the hypothesis that aberrant responses of intestinal stem cells to diet-derived mutagens may be causally involved in the restricted cancer tropism of LS. To test this we have generated a panel of isogenic mouse embryonic stem (mES) cells with heterozygous or homozygous disruption of multiple MMR genes and investigated their responses to the common dietary mutagen and carcinogen 2-amino-1-methyl-6-phenylimidazo[4,5-b]pyridine (PhIP). Our data reveal that PhIP can inactivate the wild-type allele of heterozygous mES cells via the induction of either loss of heterozygosity (LOH) or intragenic mutations. Moreover, while protective DNA damage signaling (DDS) is compromised, PhIP induces more mutations in *Msh2*, *Mlh1*, *Msh6* or *Pms2*-deficient mES cells than in wild-type cells. Combined with their spontaneous mutator phenotypes, this results in a compound hypermutator phenotype. Together, these results indicate that dietary mutagens may promote CRC development in LS at multiple levels, providing a rationale for dietary modifications in the management of LS.

Graphical Abstract

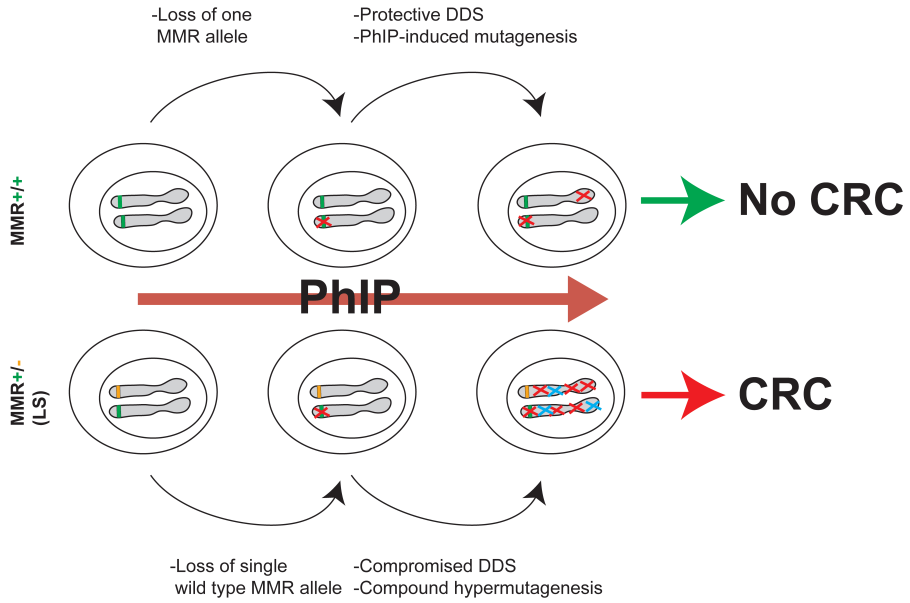

Abbreviations: CRC, colorectal cancer; LS, Lynch syndrome; MEF, mouse embryonic fibroblast; MMR, mismatch repair

Received: July 5, 2021. **Revised:** October 21, 2021. **Accepted:** November 15, 2021

Introduction

Colorectal cancer (CRC) is the third most common cancer type world-wide, with the highest incidence in developed countries (1). Many lifestyle factors increase the risk for CRC, including obesity, smoking and consumption of red, processed and cooked meat (2,3). Ten percent of all CRC has an underlying genetic predisposition. Of these, Lynch syndrome (LS) is the most prevalent (1 in 279 individuals), accounting for 3–5% of all CRCs (4). LS is caused by an inherited heterozygous defect in one of four genes involved in DNA mismatch repair (MMR), *MSH2*, *MSH6*, *MLH1* and *PMS2*. Although LS is inherited in an autosomal dominant fashion, the wild-type allele of the germ-line-defective gene must be somatically lost to procure cancer development (5).

Canonical MMR removes misincorporations by DNA polymerases during replication of undamaged DNA. Consequently, loss of MMR is associated with increased spontaneous mutagenesis. Since MMR operates in all proliferating tissues, the cause of the restricted cancer tropism of LS thus far is unclear. Interestingly, MMR-deficient cells also display aberrant mutagenic and cell cycle responses to agents that induce helix-distorting DNA lesions (6,7). This appears paradoxical since helix-distorting DNA lesions do not induce base–base mismatches, the natural substrates for MMR. Data on responses of MMR-deficient cells to UV light have suggested the involvement of MMR proteins in the removal of misincorporations induced by DNA translesion synthesis polymerases opposite helix-distorting photolesions. This prevents their mutagenicity, while simultaneously inducing protective DNA damage signaling (DDS) (7).

Heterocyclic amines are an important class of dietary genotoxic compounds, present in meat cooked at high temperatures, that induce helix-distorting nucleotide lesions. The most abundant of these heterocyclic amines is 2-amino-1-methyl-6-phenylimidazo[4,5-b]pyridine (PhIP). Indeed, dietary intake of PhIP is positively correlated with CRC (3). Here we have investigated the hypothesis that PhIP (or similar diet-derived genotoxic compounds) may direct the development of CRC in LS at three levels [see the Graphical Abstract and (7)]: (i) by inducing loss of the wild-type allele of the heterozygous MMR gene, (ii) by compromised PhIP-induced DDS in these MMR-deficient cells and (iii) by enhanced mutability of these cells by the mutagen. To address this tripartite hypothesis we have used mouse embryonic stem (mES) cells, heterozygous for *Msh2* or *Mlh1*, as models for colonic crypt stem cells in LS patients. We show that PhIP indeed induces loss of heterozygosity (LOH) or deleterious nucleotide substitutions, insertions, and deletions at the wild-type allele. Consequently, in the resulting *Msh2*-deficient mES cells, PhIP-induced DDS is reduced. Moreover, in *Msh2*-, *Msh6*-, *Mlh1*- or *Pms2*-deficient cells, the mutagenicity of PhIP is much higher than in wild-type cells. This exacerbated mutability is additive to the spontaneous mutator phenotype of MMR-deficient cells, resulting in a compound hypermutator phenotype. These results provide support for the hypothesis that intestinal mutagens are involved at multiple levels in the development of CRC in LS and suggest the feasibility of dietary intervention as a preventive approach.

Materials and methods

Cell culture and cell lines generated and used and their validation

mES cells were cultured on sub-lethally irradiated mouse embryonic fibroblast (MEF) feeder cells in complete medium consisting of KO DMEM supplemented with 10% fetal calf serum, 1% glutamax, 1% non-essential amino acids, 1mM pyruvate, 100U penicillin/100µg streptomycin, 0.1mM β-mercapto-ethanol and leukemia inhibitory factor. During experiments complete medium was mixed in a 1:1 ratio with Buffalo rat liver cell-conditioned medium (called 50/50) to allow for growth on gelatin-coated culture dishes.

Wild-type mES cell line E14 (8) was used as a parental line to all cell lines generated and used in this study (Figure 1A). The line was karyotyped before constructing derivative mutant mES cell lines. The *Msh2* and *Mlh1*-heterozygous mES cell lines used to study spontaneous and PhIP-induced loss of MMR (called Msh2-Bsd and Mlh1-Bsd) contain a *Blasticidin* selection cassette at the *Kcnk12* (3′ of the wild-type *Msh2* allele) or *Llrfip2* (3′ of the wild-type *Mlh1* allele) locus, respectively, introduced by classical gene targeting. The heterozygous *Msh2* and *Mlh1* deletions in these lines were generated using CRISPR/Cas9 (Supplementary Table 1, available at *Carcinogenesis* online; manuscript in preparation). Briefly, two complementary oligonucleotides with BbsI overhangs were annealed and ligated into CRISPR-Cas9 vector PX330-Puro. mES cells were transfected with these plasmids using Lipofectamine 2000. After transfection, the introduction of a hemizygous deletion at *Msh2* or *Mlh1* was confirmed by allele-specific PCR (see below). The presence of the *Blasticidin* cassette linked to the wild-type *Mlh1* or *Msh2* allele was validated by the appearance of clones, surviving 4 h incubation with 20µM 6-thioguanine (6tG) (Sigma–Aldrich), a hallmark of MMR deficiency (9). All these spontaneous 6tG-tolerant clones had fortuitously lost the wild-type allele by LOH and also the (linked) *Blasticidin* cassette, which resulted in re-acquired Blasticidin sensitivity (Supplementary Figure S2, available at *Carcinogenesis* online and the Results section).

The *Msh2*-1, *Msh6*-1 (10), *Mlh1*-1, *Mlh1*-s, *Pms2*-1 and *Pms2*-s knock-out cell lines (Figure 1A) have been generated using CRISPR-Cas9, as described above (Supplementary Table 1, available at *Carcinogenesis* online). After transfection, the cells were selected for tolerance of 6tG to more easily acquire MMR-deficient clones, with the exception of the *Pms2*-deficient lines that were identified by allele-specific PCR. Their phenotype was confirmed by Western blotting (Figure 1B and Supplementary Data, available at *Carcinogenesis* online only for review).

The *Msh2*-s, the *Msh6*-s and *Msh3* knock-out cell lines have been generated by conventional gene targeting (Figure 1A) and have been published before by us (11,12). All lines were validated prior to use by allele-specific PCR, as described (11,12). In addition, the *Msh2*-1 and *Msh6*-1 lines were validated prior to use by testing for 6tG tolerance and by performing Western blotting (see below; Figure 1B and Supplementary Data, available at *Carcinogenesis* online only for review). Cell lines were validated regularly by Western blotting and/or allele-specific PCR. An overview of the origin or construction of all cell lines generated and used here and their validation/authentication are provided in Supplementary Table 2, available at *Carcinogenesis* online.

Western blotting

SDS-PAGE was performed using 4–12% Criterion XT Bis-Tris gels (Bio-rad). Proteins were transferred onto Protran 0.45 µM nitrocellulose membranes (GE Healthcare). Membranes were blocked for 1 h using blocking reagent (Rockland) diluted with PBS-0.1% Tween. Then, membranes

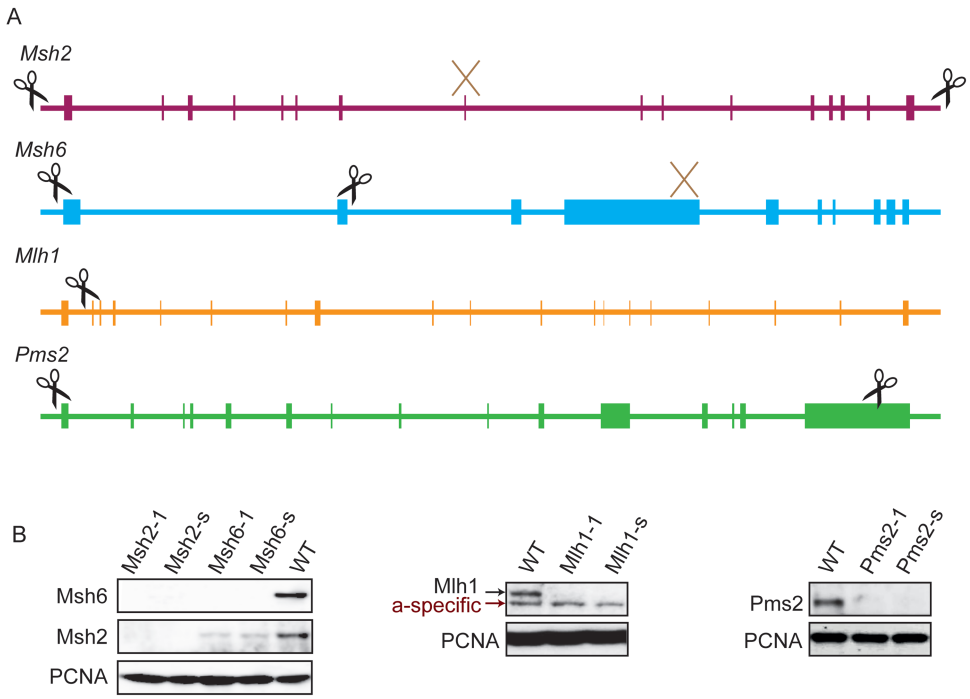

Figure 1. Canonical MMR gene alleles used in this study. (**A**) Graphical representation of the four core MMR genes. Vertical bars represent exons. Locations where guide RNAs directed a CRISPR-Cas9-induced break are symbolized by scissors. Brown crosses depict the sites where a hygromycin (*Msh2*) or puromycin (*Msh6*) resistance cassette was integrated to disrupt the gene to provide for completely independent knockouts. (**B**) Western blot validation of mES cell lines deficient for the four MMR genes. PCNA is used as a loading control. The Msh2 and Msh6 panels were derived from the same blot. The Msh2-s and Msh6-s lines were published before (9–11). Of note, some Msh2 protein is visible in the *Msh6* lines, resulting from dimerization of Msh2 with Msh3.

were incubated overnight at 4°C with primary antibodies, diluted in Rockland-PBS-Tween. Membranes were washed using PBS-Tween (0.1%) and incubated with secondary anti-mouse and anti-rabbit HRP (ThermoFisher Scientific), depending on primary antibody isotype, diluted 1:50 000 in Rockland-PBS-Tween for 1 h at room temperature. Bands were visualized using Amersham ECL select western blotting detection reagent (GE Healthcare). Antibodies used: Anti-Msh2: mouse mAb (FE11, Calbiochem), anti-Msh6 (Abcam, clone 44), anti-Mlh1: rabbit polyclonal (C-20, Santa Cruz Biotechnology), anti-Pms2: mouse Ab (A16-4, BD Pharmingen), anti-Kap-1^{p} (Bethyl, polyclonal A300-767A), anti-Chk1^{p} (clone 133D3, Cell Signaling Technology) and anti-PCNA (clone PC10 clone, Santa Cruz).

Induction of MMR deficiency by PhIP

A day prior to treatment with PhIP (Apollo Scientific) or vehicle (dimethyl sulfoxide, DMSO), 5 × 10^6 wild-type cells or cells heterozygous for *Msh2* or *Mlh1* were seeded in 50/50 medium in gelatin-coated p90 dishes. Cells were washed twice with PBS and then incubated with 18 µM PhIP or DMSO in complete medium in the presence of 10% S9 rat liver extract (Trinova), for 3 h. Subsequently, the cells were washed twice with PBS and 50/50 medium was added with or without 5 U/ml of Blasticidin (Invivogen). After two days, the cells were trypsinized and cultured for two passages to allow fixation of mutations. Afterwards, 2 × 10^6 cells were seeded in a p90 dish and the next day the cells were incubated for 4 h with 20 µM 6tG in 50/50 medium to select for MMR-deficient clones. After one week, this selection was repeated and the cells were grown for another week in 50/50 medium to allow for the formation of clones. Clones were either stained with methylene blue and counted or picked and grown until confluency in 96-well plates in the presence of 5 mM Hypoxanthine, 20 µM Aminopterin, 0.8 µM Thymidine (HAT) (50× diluted, Thermo Fisher Scientific) to select against the inadvertent loss of *Hprt* that also yields 6tG resistance (albeit to a much higher concentration).

Amplification of *Msh2* and *Mlh1* for LOH analysis

Individual clones were lysed using 50 µl DirectPCR lysis reagent (Viagen) with 8U/ml proteinase K (Invitrogen) for 1 h at 37°C. After heat inactivation of proteinase K (5 min at 85°C), one µl of cell lysate was used in a multiplex PCR with three oligonucleotide primers to analyze LOH (Supplementary Figure 1, Supplementary Table 3, available at *Carcinogenesis* online). LOH at Msh2 was analyzed using primers 1 (0.4 µM) and 2 (0.08 µM) to amplify the intact *Msh2* allele and primers 1 and 3 (0.32 µM) to amplify the disrupted *Msh2* allele. For *Mlh1*, primers 4 (0.4 µM) and 5 (0.16 µM) amplify the intact *Mlh1* allele and 4 (0.4 µM) and 6 (0.4 µM) the disrupted *Mlh1* allele. PCR products were created using GoTaq polymerase (0.625 U, Promega) in GoTaq buffer with dNTPs (0.5 mM) and primers during 35 cycles, each consisting of 30 s at 95°C, 30 s at 57°C (*Msh2*) or 61°C (*Mlh1*) and 2 min at 72°C. A final extension was performed for 10 min at 72°C. DNA products were examined using 3% agarose gel electrophoresis.

Production and sequence analysis of *Msh2* and *Mlh1* cDNA

RNA was isolated from individual clones lysed in 100 µl TRIzol reagent (Invitrogen) according to the manufacturer's protocol (TRIzol, Invitrogen). The RNA pellet was dissolved in 15 µl TE buffer and cDNA was generated using Maxima H

Minus Reverse Transcriptase (Thermo Fisher Scientific). First, a final volume of 14.5 µl containing one µl RNA, OligodT primer (6.9 µM, Thermo Fisher Scientific) and dNTPs (0.69mM, Invitrogen) was incubated for 5 min at 65°C. Then, 1 µl Maxima Polymerase (200 U/µl), 4 µl of 5× Maxima buffer and 20 U of RNAsin (Promega) were added to a final volume of 20 µl. cDNA synthesis was performed for 1 h at 57°C. After heat inactivation at 85°C for five min, cDNA was PCR amplified using GoTaq polymerase as described above with an annealing temperature of 55°C and primers 7/8 and 9/10 for the 5′ and 3′ end of *Msh2* and primers 11/12 and 13/14 for both ends of *Mlh1*. PCR products were analyzed using 2% agarose gel electrophoresis. PCR products were purified using a QIAquick PCR purification kit (Qiagen) following manufacturer's protocol and eluted in a final volume of 20 µl deionized H_2O. Five microlitres of purified PCR product was used for Sanger sequencing using 1.25 µM of primer 8/10/12/15 for the 5′ and 3′ end of *Msh2* and *Mlh1*, respectively. Sequences were analyzed using ContigExpress from VectorNTI Suite 9. Primer sequences are listed in Supplementary Table 3, available at *Carcinogenesis* online.

Analysis of pathogenicity of PhIP-induced *Msh2* and *Mlh1* mutations

To analyze whether PhIP-induced mutations in MMR heterozygous mES cells reflect pathogenic mutations in humans, we used a combination of an *in silico* analysis (13), databases used for the classification of human MMR variants (ClinVar (14), InSiGHT (15) and COSMIC (16)), and two functional assays (CIMRA (17,18) and reverse diagnosis catalogues ((19,20), manuscript in preparation). For *in silico* analyses a probability of pathogenicity of less than 0.1 and more than 0.9 were used for classification as likely pathogenic or benign, respectively (13). Insertions/deletions that caused frameshifts were also classified as pathogenic, while in frame insertion/deletions are categorized as unknown.

Analysis of PhIP-induced toxicity and DDS

mES cells were seeded at a density of 5×10^4 cells per well of a 6-well plate, one day before treatment with a dose-range of 0–25 µM PhIP, as described above. Cells were grown in 50/50 medium for 4 days post-treatment. The number of surviving cells was counted using a Beckman coulter counter.

The induction of DDS by PhIP was assessed as follows: one day prior to treatment with 18 µM PhIP or vehicle for 1 h, 1×10^6 wild-type and *Msh2*-deficient cells were seeded per well of a 6-well plate. PhIP/vehicle treatment was performed as described above. After two washes of PBS, cells were grown for another 2 h (PhIP) or 5 h (PhIP or vehicle) in 50/50 medium before lysates were made in Laemmli sample buffer, gel electrophoresis and W blotting, as described above.

Determination of *Hprt*-mutant frequencies

mES cells were grown in HAT-supplemented 50/50 medium for six days to eliminate pre-existing *Hprt*-mutant cells. Then, 5×10^6 cells were seeded in p90 dishes, one day prior to PhIP or mock treatment. PhIP (18 µM) or mock treatment was performed as described above. Next, 5×10^6 cells were seeded in gelatin-coated p90 dishes and grown for six days in 50/50 medium to allow fixation of mutations. Next, 2×10^6 cells were grown 50/50 medium supplemented with 6tG (30 µM) to select *Hprt* deficient clones. In parallel, 3×250 cells were seeded in 50/50 medium in p60 dishes to determine cloning efficiencies. After 7–10 days, clones were stained with methylene blue and the *Hprt*-mutant frequency was calculated by determining the number of 6tG-resistant clones divided by the total number of clone-forming cells seeded in 6tG containing medium.

Next-generation sequencing of *Hprt*-mutant clones

Approximately 400 6tG-resistant clones from PhIP-treated wild-type and *Msh2*-deficient mES cell cultures and 400 6tG-resistant clones from mock-treated *Msh2* deficient ES cells were used for Next Generation Sequencing (NGS). Per experimental condition clones were pooled and cells were lysed with 1.6 ml TRIzol reagent for total RNA isolation. A baseline wild-type sequence was established from 8×10^6 cells, corresponding to the total number of cells of 400 6tG-resistant clones. *Hprt* cDNA was generated using Maxima Reverse Transcriptase (ThermoFisher Scientific) and *Hprt*-specific oligonucleotide primer 21. PCR products for NGS were generated in a two-step procedure. First, three separate PCRs were performed using primer combinations 16/17, 18/19 and 20/21 to amplify three overlapping amplicons of the *Hprt* cDNA. The reaction mixture of 40 µl consisted of Phusion High-Fidelity DNA polymerase (0.4U) (Thermo Fisher Scientific), Phusion polymerase reaction buffer, dNTPs (0.4 µM), Forward primer (0.5 µM), Reverse primer (0.5 µM) and 2 µl cDNA. Using a thermocycler, PCR products were generated by incubating the reaction mixture for 2 min at 95°C, followed by 15 s at 95°C, 30 s at 57°C and 1 min 72°C for 25 cycles, and a final elongation step of 72°C for 5 min. PCR products were purified using AMPure XP beads (Beckman Coulter) following manufacturer's protocol and eluted in 20 µl deionized H_2O. Subsequently, another Phusion PCR was performed as previously described with the exception of cycling for 8 PCR cycles instead of 25. For this PCR, forward (21–24) and reverse (25–28) primers were used with unique barcodes for each condition (Supplementary Table 3, available at *Carcinogenesis* online). Following purification using AMPure beads, the size of each PCR product was assessed using a Qiaxcel Advanced System (Qiagen). Finally, 50ng pooled PCR products was sequenced using Illumina Paired-End sequencing (GenomeScan).

Analysis of spectra of PhIP-induced mutations in the *Hprt* coding region

To detect alterations in cDNA the paired-end data was first filtered to contain exclusively high-quality reads. Thus, only reads with a maximum error probability of 0.05 were kept. Paired-end reads were merged using Flash (29) and mapped to the *Hprt* reference sequence using in-house software (van Schendel *et al.* manuscript in preparation). Additional filtering was applied to ensure each read started and ended with the primer combinations used (see above). Finally, each mapped read was compared to the reference *Hprt* sequence and annotated into wild-type (no difference compared to reference), single nucleotide substitution, multi nucleotide substitution, deletion or insertion. To identify unique mutations from background noise we considered mutations to be real if the allele frequency was >0.001.

Results

An isogenic set of MMR gene-disrupted mES cells

mES cells are primary, diploid and display strong DNA damage responses, thus providing good models for intestinal stem

cells in LS patients. We have previously described the *Msh2*-s, Msh6-1 and *Msh6*-s lines (10–12).

Since the mutator phenotype conferred by MMR deficiency predisposes to genetic drift, we decided to also use independently constructed isogenic mES cell lines, each carrying a targeted disruption of both alleles of one of the four genes MMR (Figure 1A). These cell lines were generated using CRISPR-Cas9, as described in the Materials and Methods section, resulting in cell lines called *Msh2*-1, *Mlh1*-1, *Mlh1*-s, *Pms2*-1 and *Pms2*-s (Figure 1B). As models for MMR gene-heterozygous colonic stem cells in LS patients, we employed recently generated mES cell lines, heterozygous for *Msh2* or for *Mlh1*. In these cells, the wild-type *Msh2* or *Mlh1* allele was flanked by a *Blasticidin* resistance cassette (M. Drost et al, in preparation; Figure 2A). This *Blasticidin* resistance cassette enables us to distinguish between clones that have lost the wild-type allele by an intragenic mutation, since these retain the linked cassette, and clones that have undergone LOH, which results in concomitant loss of Blasticidin resistance. Thus, these cells allow to sensitively investigate the mechanistic basis of loss of the wild-type allele in MMR gene-heterozygous cells.

PhIP induces MMR deficiency in MMR gene-heterozygous cells

Loss of the single functional MMR allele resulting from intragenic mutations or LOH is a prerequisite for the development of CRC in LS individuals (21). We investigated whether, and how, PhIP can induce loss of the wild-type allele of a heterozygous MMR gene by using the *Blasticidin* cassette-tagged mES cells, heterozygous for *Msh2* or *Mlh1*. We exploited the acquired tolerance of MMR-deficient cells to the nucleoside analog 6-thioguanine (6tG; Figure 2A, Supplementary Figure S1, available at *Carcinogenesis* online) to select individual clones that have lost the wild-type allele in a MMR gene-heterozygous mES cell line (9). 6tG selection was followed by HAT counterselection to eliminate cells that inadvertently have acquired 6tG resistance by an inactivating mutation in the *Hprt* gene.

In the absence of PhIP treatment, selection of *Msh2* or *Mlh1*-heterozygous mES cell lines with 6tG yielded clones, suggesting a significant frequency of spontaneous loss of the wild-type allele (Figure 2B). These clones had all become Blasticidin-sensitive, indicating that the wild-type allele occasionally is lost by LOH, in the absence of a mutagen (Figure 2C). Exposure to PhIP significantly increased the frequency of 6tG-tolerant clones in each heterozygous mES cell line (Figure 2B–D, Supplementary Table S1, available at *Carcinogenesis* online), suggesting that PhIP induces increased loss of the wild-type allele. Of note, the frequency of both spontaneous and PhIP-induced loss of the wild-type allele in *Msh2*-heterozygous cells was higher than that in *Mlh1*-heterozygous cells. This was not a consequence of higher 6tG tolerance, and therefore of more efficient selection, of *Msh2*-deficient than of *Mlh1*-deficient cells (Supplementary Figure S1, available at *Carcinogenesis* online). Thus, we infer that both spontaneous and PhIP-induced allelic loss is more efficient at *Mhs2* than at *Mlh1*. In each cell line, approximately 75% of the PhIP-induced 6tG-tolerant clones were Blasticidin-sensitive, indicating that PhIP predominantly induces LOH at the wild-type allele. Nevertheless, about 25% of the PhIP-induced 6tG-tolerant clones had retained Blasticidin resistance, suggesting that in these clones the wild-type allele was lost by a PhIP-induced intragenic mutation. To provide more evidence for the latter, we performed an allele-specific multiplex PCR on isolated clones. Indeed, all Blasticidin-resistant clones had retained one allele of *Msh2* or *Mlh1*, whereas the majority of the Blasticidin-unselected clones had undergone complete loss of the wild-type allele, confirming the induction of LOH by PhIP (Supplementary Figure S2, available at *Carcinogenesis* online).

Inactivation of the wild-type allele in MMR-heterozygous cells by PhIP-induced mutations

To confirm that in these 6tG-selected, Blasticidin-resistant, clones the wild-type *Msh2* or *Mlh1* allele was inactivated by a PhIP-induced intragenic mutation, Sanger sequencing was performed on cDNA. The results showed that for both genes the spectrum of PhIP-induced mutations consisted mostly of single nucleotide substitutions (SNS) and intragenic deletions (Supplementary Tables S2 and S3, available at *Carcinogenesis* online). All deletions started at a guanine and SNS were dominated by G.C > T.A transversions. These data are consistent with the adduct spectrum of PhIP (typically at G nucleotides) and its mutational fingerprint (22,23). The mutations were distributed over *Msh2* and *Mlh1* (Supplementary Figure S3, available at *Carcinogenesis* online). To confirm that the mutations resulted in inactivation of the wild-type allele of these genes we used *in silico* analyses, data derived from functional assays, and variant databases. These databases list human variants and thus only mutations of residues conserved between mouse and human DNA could be studied (Supplementary Tables S2 and S3, available at *Carcinogenesis* online). In particular, an SNS was deemed likely pathogenic in case (i) the *in silico* predicted probability of pathogenicity (13) exceeded 0.9, (ii) when MMR functionality was compromised in functional assays such as the biochemical MMR (CIMRA) assay (17,18), (iii) when the mutation was identified by large-scale genetic screens for deleterious variants [(19,20), manuscript in preparation], (iv) when identified in LS patients as likely pathogenic or pathogenic in the ClinVar (14) or InSiGHT (15) databases, (v) when listed in the COSMIC cancer somatic database (16). Seven out of 8 and 8 out of 12 SNS in *Msh2* and *Mlh1*, respectively, comprised conserved residues and 7/7 and 6/8, respectively, were predicted pathogenic using the aforementioned analyses (Figure 2E, Supplementary Tables S2 and S3, available at *Carcinogenesis* online). Only in *Mlh1*, two substitutions could not be classified while none of the PhIP-induced substitutions in either gene were predicted to be benign. In addition, almost all intragenic deletions that we identified were either large in size and/or frameshifting and thus also deemed pathogenic. Combined, these data show that MMR gene-heterozygous stem cells lose their wild-type MMR gene by spontaneous LOH and, at a high frequency, by PhIP-induced LOH or intragenic mutations.

MMR deficiency leads to impaired DDS in response to PhIP treatment

To test whether the MMR status affects the toxicity of PhIP, survival of isogenic mES cells, defective for any of the four canonical MMR genes, was determined following exposure to a dose range of PhIP. No significant difference in survival between wild-type and MMR-deficient lines *Msh2-1*, *Msh6-1*, *Mlh-1* and *Pms2-1* was found (Figure 3A). Then, we assessed the induction of DDS by PhIP in wild-type and *Msh2*-deficient mES cells. This was done by western blotting using antibodies against phosphorylated Chk1 and Kap-1, DDS markers for

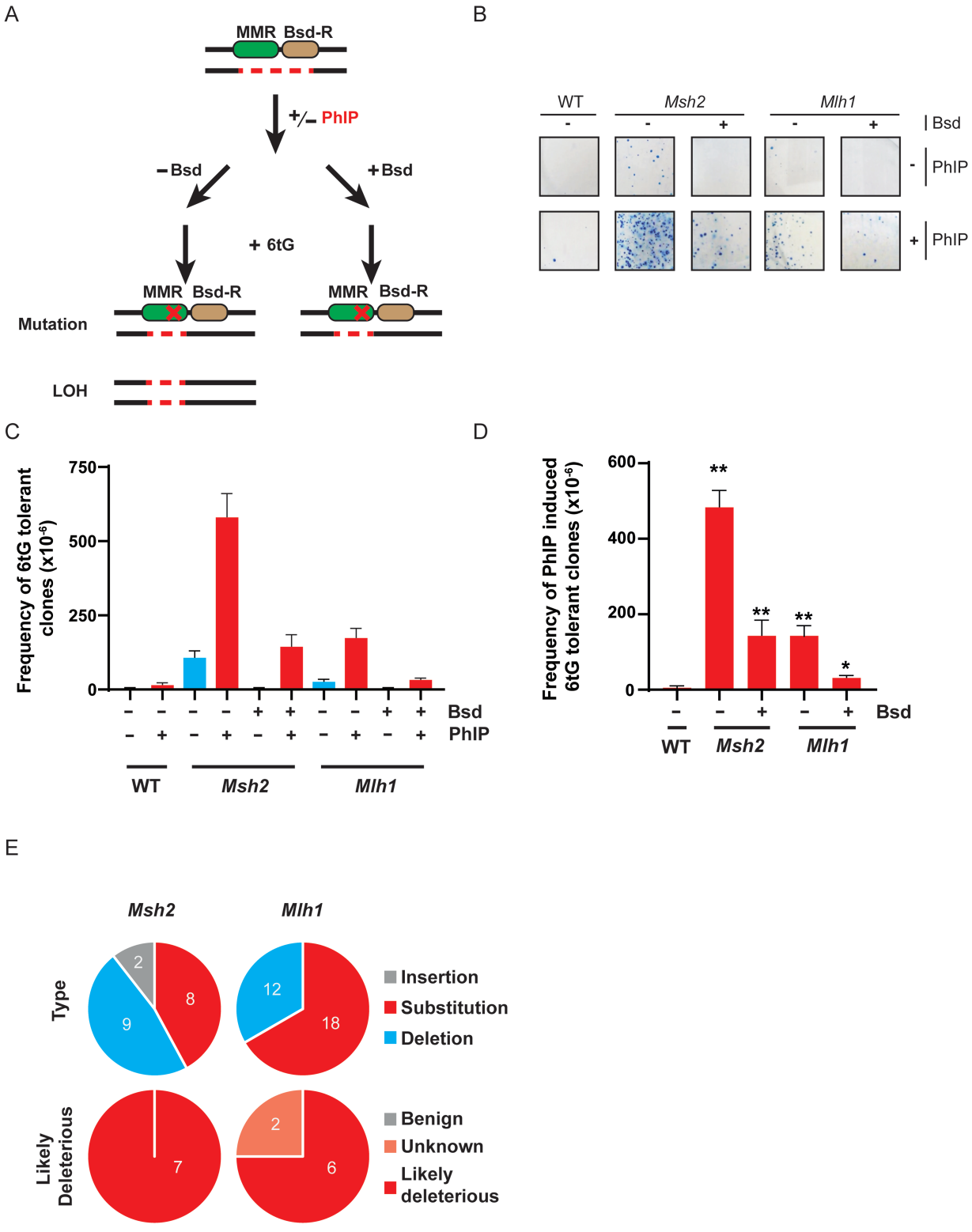

Figure 2. PhIP-induces loss of MMR in MMR gene-heterozygous mES cells. (**A**) Selection pipeline to investigate PhIP-induced loss of MMR in MMR gene-heterozygous cells. One allele of either *Msh2* or *Mlh1* was deleted using CRISPR-Cas9 in mES cells (red dashes) whilst the wild-type allele was marked at the 3′ side with a *Blasticidin* resistance gene (Bsd-R). These cell lines were treated with PhIP to investigate the induction of loss of the wild-type allele by either an intragenic mutation (which leads to preservation of Bsd resistance) or by loss of heterozygosity (LOH, which results in concomitant loss of the Bsd-R gene). 6tG was used to select for MMR-deficient cells, with or without concomitant Bsd selection. (**B**) Wild-type, *Msh2* and *Mlh1*-heterozygous cells were exposed to PhIP or vehicle, cultured for a week, and treated with 6tG. Surviving clones were stained with methylene blue. (**C**) Spontaneous or PhIP-induced MMR-deficient clones ($n = 3$). Half of the plates were also treated with Blasticidin (Bsd) to select for intragenic events. Error bars, SEM. (**D**) PhIP-induced MMR-deficient clones (after subtraction of spontaneous MMR-deficient clones). Error bars, SEM. $*P \leq 0{,}05$, $**P \leq 0{,}01$; unpaired *T*-test of groups compared to WT. (**E**) Upper panel: PhIP-induced mutations in *Msh2* and *Mlh1* cDNA. Lower panel: predicted pathogenicity of PhIP-induced substitution mutations. Number, number of clones.

the formation of single-stranded and double-stranded DNA breaks, respectively. In wild-type cells, both markers were increased at 3 and 6 h post PhIP addition. Deficiency of *Msh2* resulted in a significant mitigation of Kap-1 phosphorylation and a, less pronounced, decrease in Chk1 phosphorylation (Figure 3B). These data indicate that *Msh2* is involved in provoking DDS induced by PhIP, which suggests that *Msh2*-deficient stem cells might partially have lost protective checkpoint responses to intestinal mutagens, a result consistent with the previously observed dependence on *Msh2* of DDS and checkpoint responses induced by UV-induced DNA damage (7).

MMR-deficient cells are hypermutable by PhIP

To investigate whether the mutagenicity of PhIP is affected by MMR deficiency we quantified the frequency of mutations induced by PhIP in wild-type and the mES cell lines *Msh2-1*, *Msh6-1*, *Mlh1-1* and *Pms2-1*, using the *Hprt* gene as a reporter (Figure 3C–D, and Supplementary Figures S4A and S4B, available at *Carcinogenesis* online for independent cell lines). Similar to selection of MMR-deficient clones (see above), selection for mutational inactivation of *Hprt* employs 6tG although, rather than by a pulse, selection for deleterious *Hprt* mutations is continuous and uses a higher dose. Almost no *Hprt*-mutant clones were found in vehicle-treated wild-type cells or cells deficient for the minor MMR gene *Msh3*, an alternative binding partner of Msh2 involved in repairing relatively large insertion/deletion loops (24) (Figure 3C). PhIP treatment of these cell lines yielded a moderate increase of the mutant frequencies ranging between approximately 10 and 20 × 10^{-6} mutants (Figure 3D). Whereas the MMR-deficient cell lines displayed spontaneous mutant frequencies varying between 45 and 110 × 10^{-6}, higher frequencies of *Hprt*-mutant clones were obtained following PhIP treatment of these cell lines (approximately 220 × 10^{-6}; Figure 3C). Subtracting the *Hprt* mutant frequencies of the vehicle-treated cells from those of the PhIP-treated cells revealed that PhIP induced much higher frequencies of mutants in all MMR-deficient cells than in wild-type or *Msh3*-deficient cells (Figure 3D). Importantly, by using a completely independent set of isogenic mES cell lines *Msh2-s*, *Msh6-s*, *Mlh1-s* and *Pms2*-s) we obtained identical results (Supplementary Figure S4, available at *Carcinogenesis* online), excluding that secondary mutations are responsible in the observed phenotypes. Thus, in addition to suppressing the mutagenicity of spontaneous replication errors, MMR genes suppress the induction of mutations by

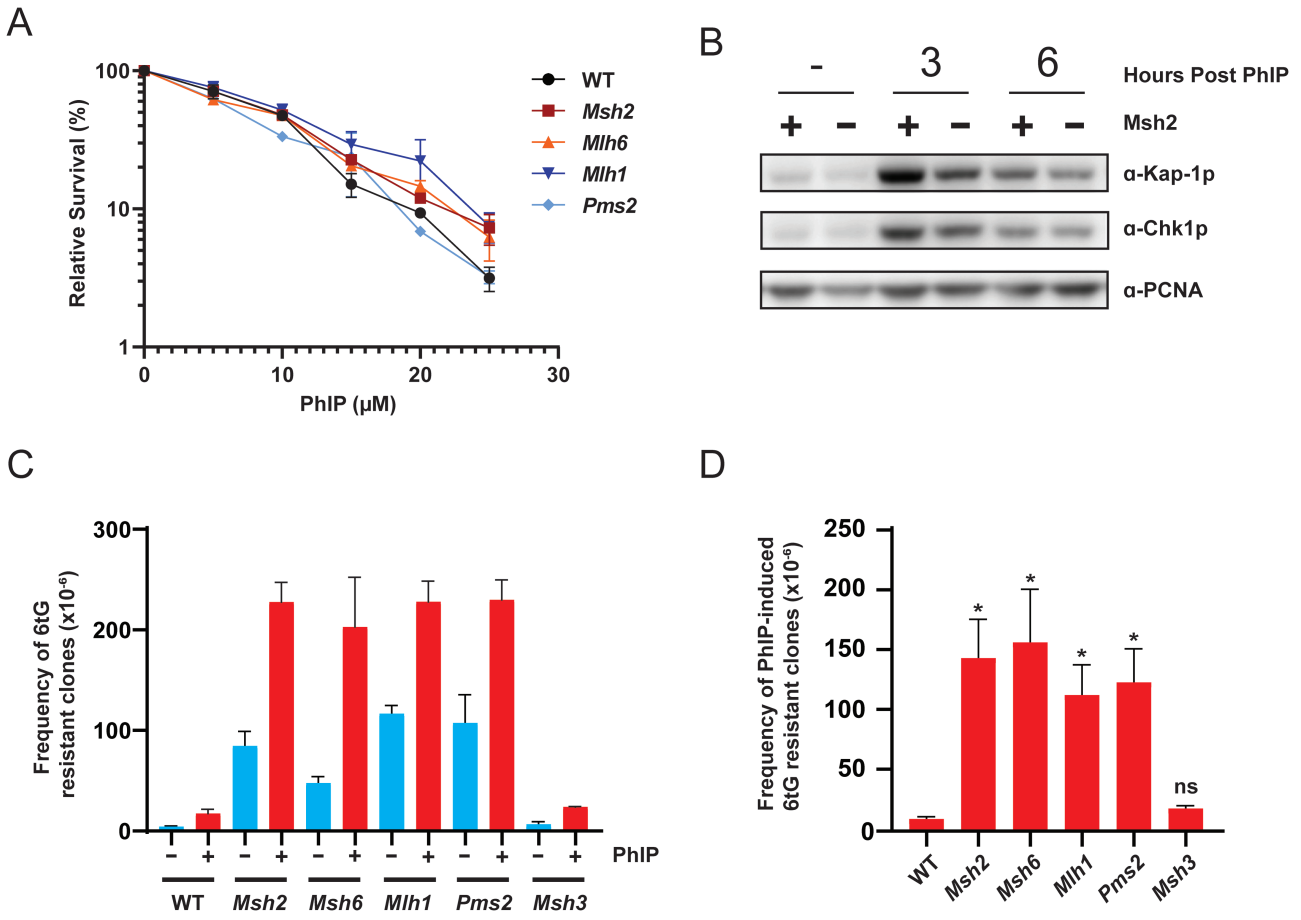

Figure 3. MMR deficient cell lines Msh2-1, Msh6-1, Mlh-1 and Pms2-1 are hypermutable and display reduced DDS following PhIP exposure. (**A**) Cell survival after 5 days following exposure to a dose range of PhIP (n = 3). Error bars, SEM. (**B**) Western blot probing for the DDS markers phosphorylated Kap-1 and phosphorylated Chk1. PCNA is used as loading control. Representative image of 3 independent experiments. (**C**) Frequency of *Hprt* mutants in isogenic MMR-proficient and -deficient mES cell lines following mock or PhIP treatment (n = 3). Error bars, SEM. See Supplementary Figure S4, available at *Carcinogenesis* online for experiments using independent MMR gene mutants. (**D**) Frequency of *Hprt*-mutant clones induced by PhIP treatment (corrected for spontaneous mutants). Error bars, SEM. *$P \leq 0.05$, ns, not statistically significant; unpaired T-test comparing groups to wild-type.

PhIP. We conclude that the combination of spontaneous and enhanced PhIP-induced mutagenesis in MMR-deficient cells procures a compound hypermutator phenotype.

PhIP-induced mutant spectra in wild-ype and MMR-deficient cells

To investigate whether MMR genes, in addition to suppressing PhIP-induced mutations, also affect the PhIP-induced mutation spectrum we treated wild-type and *Msh2-1* cells with PhIP or vehicle, selected for *Hprt* mutants, and sequenced pooled *Hprt* cDNAs using an amplicon based next-generation sequencing approach to analyze most of the *Hprt* cDNA. Using a novel sequencing analysis pipeline (R. van Schendel, manuscript in preparation), 58 unique mutations in PhIP treated wild-type cells, 49 mutations in mock-treated *Msh2*-deficient cells and 58 mutations in PhIP treated *Msh2*-deficient cells were identified at a 0,1% cut-off for allele frequency (Supplementary Tables S4–S6, available at *Carcinogenesis* online). Only one spontaneous mutation was found in mock-treated wild-type samples, confirming minimal sequencing noise.

In both wild-type and *Msh2*-deficient cells, 75% of both spontaneous and PhIP-induced mutations were SNS (Figure 4A). To a lesser extent, *Hprt* was inactivated by multi nucleotide substitutions (MNS, e.g. CGAT > ATTA), insertions and deletions. MNS were exclusively found in cells treated with PhIP, whereas insertions were associated with loss of *Msh2*. By multiplying the fractions of the SNS spectra (Figure 4A) with the absolute mutant frequencies that were obtained earlier for mock and PhIP-exposed conditions (Figure 3C, D) we then obtained the frequency of each type of spontaneous and PhIP-induced nucleotide substitution in both cell lines (Figure 4B and C, Supplementary Table S7, available at *Carcinogenesis* online). In wild-type cells most PhIP-induced SNSs were G.C > T.A transversions, at a frequency of 12.2×10^{-6}. In mock-treated *Msh2*-deficient cells, spontaneous SNS consisted mostly of G.C > A.T and A.T > G.C transitions (at a frequency of 25.7×10^{-6} each). In *Msh2*-deficient cells treated with PhIP, mutations were mainly comprised of 104.9×10^{-6} G.C > T.A transversions, 74.0×10^{-6} G.C > A.T transitions and 61.7×10^{-6} A.T > G.C transitions. Other substitutions were very rare. Spectra of PhIP-induced SNS were determined by correcting spectra obtained after PhIP treatment for the spontaneous spectra (Figure 4C). This revealed that *Msh2* specifically suppresses PhIP-induced G.C >T.A transversions, the dominant SNS type also induced in wild-type cells. Interestingly, also the frequencies of G.C > A.T and A.T > G.C transitions, that are also part of the spontaneous mutation spectrum in MMR-deficient cells (Figure 4B), were increased following PhIP treatment. Finally, in both PhIP-treated wild-type and *Msh2*-deficient cells there was a strong bias towards nucleotide substitutions derived from guanines in the nontranscribed strand (Supplementary Figure S5, available at *Carcinogenesis* online), consistent with the removal of most PhIP-adducted nucleotides from the transcribed strand by transcription-coupled nucleotide excision repair, which precludes their mutagenicity.

Discussion

Here we have generated and used isogenic panels of mES cells with targeted heterozygous deficiencies in the MMR genes *Msh2* or *Mlh1* or homozygous deficiencies in *Msh2*, *Msh6*, *Mlh1*, *Pms2* or *Msh3* as models for intestinal stem cells in LS patients and investigated responses of these cells to the prototypic heterocyclic amine PhIP.

While spontaneous LOH in *Msh2* or *Mlh1*-heterozygous cell lines was readily detectable, in both genotypes frequencies of loss of the wild-type allele were strongly increased by a single exposure to PhIP (Figure 2B–D). Compared with *Msh2*-heterozygous cells, a lower number of MMR-deficient colonies were obtained following PhIP treatment of *Mlh1*-heterozygous cells, possibly reflecting locus-specific differences in allelic loss. The presence of a *Blasticidin* resistance cassette, linked to the wild-type *Msh2* or *Mlh1* allele in these cell lines, allowed us to directly distinguish between either loss of the wild-type allele by LOH (25), or by an intragenic deleterious mutation. Indeed, in approximately 25% of all MMR-deficient clones, PhIP treatment had induced inactivation of the wild-type allele of *Msh2* or *Mlh1* by an intragenic mutation (Fig. 2D, Supplementary Figure S2, available at *Carcinogenesis* online). The spectrum of these intragenic

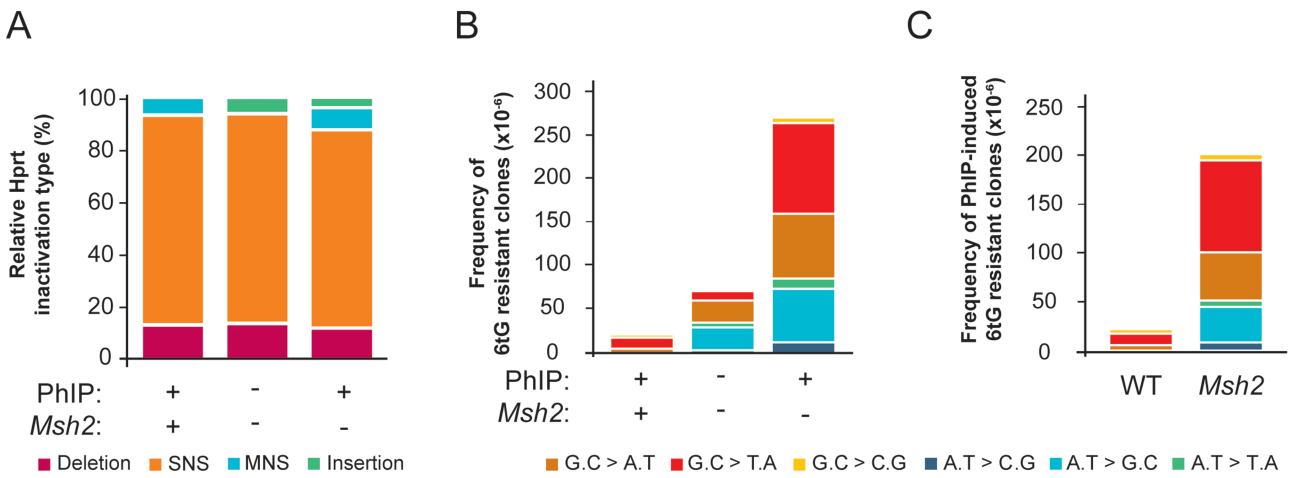

Figure 4. Analysis of PhIP-induced mutations at Hprt in MMR-proficient and -deficient backgrounds. (**A**) Percentage of *Hprt* mutants by event type, relative to the total number of unique mutants per condition. SNS, single nucleotide substitution. MNS, multi nucleotide substitution. (**B**) Distribution of different single nucleotide substitutions. (**C**) Contribution of different nucleotide substitutions to PhIP-induced *Hprt*-mutant clones.

mutations is dominated by G.C > T.A transversions, in line with the spectrum induced by PhIP (22,23,26–28,30). Using a variety of analytical approaches we confirmed that the SNS induced by PhIP in the wild-type *Msh2* or *Mlh1* allele disrupt gene function (Figure 2E). In support with the involvement of dietary mutagens in the induction of loss of MMR in the intestine of LS patients, our findings reflect observations in MMR-deficient tumors in LS patients where loss of the wild-type allele frequently is caused by LOH (31,32) while MMR inactivation by SNS also occurs albeit at a lower frequency (33). Importantly, deleterious SNS might not result in loss of protein expression *per se*, which warrants caution as to the use of immunohistochemical staining for loss of MMR gene expression in CRC as a criterium to screen for MMR gene mutations in individuals suspected of LS (34).

Loss of DDS, that mediate protective checkpoint responses, senescence or apoptosis, is a prerequisite for early steps of carcinogenesis (35). Previous work has shown that loss of *Msh2* results in defective DDS in response to DNA damage induced by methylating agents and UV light (7,36). We show here that also in response to PhIP, DDS of double-stranded DNA breaks (phospho-Kap-1) or (albeit to a lesser extent) persistent single stranded DNA (phospho-Chk1) partially depends on the MMR status (Figure 3B). After exposure to a single dose of UV light, MMR-deficient cells displayed enhanced cell cycle progression compared with MMR-proficient cells (7). However, we did not observe a similar response after PhIP exposure (not shown), indicating that cell cycle responses to PhIP may only weakly be dependent on the MMR status. Nevertheless, the observed defective DDS might provide a long-term selective advantage of MMR-deficient over heterozygous intestinal stem cells when chronically exposed to PhIP or other diet-derived genotoxic agents.

Previously, we have found that *Msh2*- and *Msh6*-deficient cells are hypermutable by UV light (7,9), possibly by correcting misincorporations opposite photolesions by mutagenic translesion synthesis polymerases (37). Here we found that also the frequencies of PhIP-induced mutations are significantly higher in cells deficient for any of the four core MMR genes than in wild-type cells (Figure 3D and Supplementary Figure S3, available at *Carcinogenesis* online). This exacerbated mutagenicity of helix-distorting nucleotide lesions acts in conjunction with the spontaneous mutagenesis in MMR-deficient cells, resulting in a compound hypermutagenesis phenotype. Importantly, these results were fully reproducible in an independent set of mutant cell lines (Supplementary Figure S4, available at *Carcinogenesis* online). Mutational spectra analysis revealed that the frequency of the prevalent SNS induced by PhIP in wild-type cells, G.C > T.A transversions, was increased most strongly in the absence of *Msh2* (Figure 4C). This result suggests that MMR directly suppresses the mutagenicity of PhIP, possibly by removing misincorporations by translesion synthesis opposite the major lesion, dG-C8-PhIP-adducted guanines (30). This would be analogous to the proposed removal of misincorporations generated by translesion synthesis opposite UV light-induced photolesions (7).

G.C > A.T and A.T > G.C transitions dominate the spontaneous mutant spectrum of *Msh2*-deficient cells (Figure 4B). Surprisingly, although these transitions do not represent typical PhIP-induced substitutions in wild-type cells, their frequency was increased by PhIP treatment of *Msh2*-deficient cells (Figure 4B, C). This might reflect the efficient activity of MMR at translesion synthesis-dependent misincorporations opposite PhIP-induced nucleotide adducts. Alternatively, the reduced DDS in the Msh2-deficient cells (Figure 3B) might enable the survival of cells carrying excessive numbers of misincorporations by translesion synthesis, that otherwise would be eliminated by apoptosis. The wild-type survival of *Msh2*-deficient cells in response to PhIP (Figure 3A), however, argues against this possibility. Finally, it cannot be excluded that in the absence of *Msh2*, mutagenic translesion synthesis is deregulated, as suggested previously (38), leading to more misincorporations in response to PhIP treatment. Irrespective of the underlying mechanism, these data show that PhIP is significantly more mutagenic in MMR-deficient cells than in MMR-proficient cells.

Taken together, our data support the possibility that dietary mutagens such as PhIP may direct CRC in LS patients at multiple levels (see the Graphical Abstract). First, PhIP exposure increases the frequency of somatic inactivation of the wild-type allele in MMR-heterozygous cells by LOH or by a nucleotide substitution, resulting in MMR deficiency (Graphical Abstract). Second, the resulting MMR-deficient cells can no longer efficiently activate protective DDS in response to PhIP (Figure 3B). Last, exposure of such MMR-deficient cells to PhIP results in compound hypermutagenesis resulting from both the spontaneous mutator phenotype at undamaged nucleotides associated with MMR deficiency (Figure 3C, blue bars) as well as with the strongly increased mutability of these cells by PhIP as compared with wild-type cells (Figure 3D). Following validation of these observations in *in vivo* models, our findings may provide a rationale for dietary modification as a preventative strategy for LS-associated CRC.

Supplementary material

Supplementary data are available at *Carcinogenesis* online.

Funding

The Netherlands Organization for Scientific Research (ALWOP 131) to N.d.W. and R.Ij.

Acknowledgements

The authors acknowledge Prof. Marcel Tijsterman for discussions and Dr Robin van Schendel for his invaluable help with the next-generation sequencing analysis. The authors also thank Jente M. Houweling MSc, Renuka P.E. Ramlal BSc, Gido Snaterse MSc and Yvonne Tiersma MSc for generating cell lines and for experimental assistance.
Conflict of Interest Statement: None declared.

References

1. IARC. *Globocan 2018: Cancer Fact Sheets—Colorectal Cancer* http://gco.iarc.fr/today/data/factsheets/cancers/10_8_9-Colorectum-fact-sheet.pdf2018
2. Derry, M.M. *et al.* (2013) Identifying molecular targets of lifestyle modifications in colon cancer prevention. *Front. Oncol.*, 3, 119.
3. Chiavarini, M. *et al.* (2017) Dietary intake of meat cooking-related mutagens (HCAs) and risk of colorectal adenoma and cancer: a systematic review and meta-analysis. *Nutrients.*, 9, 514.
4. Win, A.K. *et al.* (2017) Prevalence and penetrance of major genes and polygenes for colorectal cancer. *Cancer Epidemiol. Biomarkers Prev.*, 26, 404–412.

5. Lynch, H.T. *et al.* (2015) Milestones of Lynch syndrome: 1895–2015. *Nat. Rev. Cancer*, 15, 181–194.
6. Ijsselsteijn, R. *et al.* (2020) DNA mismatch repair-dependent DNA damage responses and cancer. *DNA Repair (Amst).*, 93, 102923.
7. Tsaalbi-Shtylik, A. *et al.* (2015) Excision of translesion synthesis errors orchestrates responses to helix-distorting DNA lesions. *J. Cell Biol.*, 209, 33–46.
8. Hooper, M. *et al.* (1987) HPRT-deficient (Lesch-Nyhan) mouse embryos derived from germline colonization by cultured cells. *Nature,* 326, 292–295.
9. Borgdorff, V. *et al.* (2005) Spontaneous and mutagen-induced loss of DNA mismatch repair in Msh2-heterozygous mammalian cells. *Mutat. Res.*, 574, 50–57.
10. Van Gool, I.C. *et al.* (2018) Adjuvant treatment for POLE proofreading domain-mutant cancers: sensitivity to radiotherapy, chemotherapy, and nucleoside analogues. *Clin. Cancer Res.*, 24, 3197–3203.
11. de Wind, N. *et al.* (1995) Inactivation of the mouse Msh2 gene results in mismatch repair deficiency, methylation tolerance, hyperrecombination, and predisposition to cancer. *Cell*, 82, 321–330.
12. de Wind, N. *et al.* (1999) HNPCC-like cancer predisposition in mice through simultaneous loss of Msh3 and Msh6 mismatch-repair protein functions. *Nat. Genet.*, 23, 359–362.
13. Thompson, B.A. *et al.* (2013) Calibration of multiple in silico tools for predicting pathogenicity of mismatch repair gene missense substitutions. *Hum. Mutat.*, 34, 255–265.
14. Landrum, M.J. *et al.* (2018) ClinVar: improving access to variant interpretations and supporting evidence. *Nucleic Acids Res.*, 46, D1062–D1067.
15. Thompson, B.A. *et al.* (2014) Application of a 5-tiered scheme for standardized classification of 2,360 unique mismatch repair gene variants in the InSiGHT locus-specific database. *Nat. Genet.,* 46, 107–115.
16. Tate, J.G. *et al.* (2019) COSMIC: the Catalogue Of Somatic Mutations In Cancer. *Nucleic Acids Res.*, 47, D941–D947.
17. Drost, M. *et al.* (2012) A rapid and cell-free assay to test the activity of lynch syndrome-associated MSH2 and MSH6 missense variants. *Hum. Mutat.*, 33, 488–494.
18. Drost, M. *et al.* (2010) A cell-free assay for the functional analysis of variants of the mismatch repair protein MLH1. *Hum. Mutat.*, 31, 247–253.
19. Drost, M. *et al.* (2013) Genetic screens to identify pathogenic gene variants in the common cancer predisposition Lynch syndrome. *Proc. Natl. Acad. Sci. USA*, 110, 9403–9408.
20. Drost, M. *et al.* (2020) Two integrated and highly predictive functional analysis-based procedures for the classification of MSH6 variants in Lynch syndrome. *Genet. Med.*, 22, 847–856.
21. Sekine, S. *et al.* (2017) Mismatch repair deficiency commonly precedes adenoma formation in Lynch syndrome-associated colorectal tumorigenesis. *Mod. Pathol.*, 30, 1144–1151.
22. Zhang, S. *et al.* (2001) Msh2 DNA mismatch repair gene deficiency and the food-borne mutagen 2-amino-1-methy1-6-phenolimidazo [4,5-b] pyridine (PhIP) synergistically affect mutagenesis in mouse colon. *Oncogene*, 20, 6066–6072.
23. Smith-Roe, S.L. *et al.* (2006) Mlh1-dependent suppression of specific mutations induced *in vivo* by the food-borne carcinogen 2-amino-1-methyl-6-phenylimidazo [4,5-b] pyridine (PhIP). *Mutat. Res.*, 594, 101–112.
24. Genschel, J. *et al.* (1998) Isolation of MutSβ from human cells and comparison of the mismatch repair specificities of MutSβ and MutSα. *J. Biol. Chem.*, 1998;273:19895–19901.
25. Thiagalingam, S. *et al.* (2001) Mechanisms underlying losses of heterozygosity in human colorectal cancers. *Proc. Natl. Acad. Sci. USA*, 98, 2698–2702.
26. Lynch, A.M. *et al.* (1998) Genetic analysis of PHIP intestinal mutations in MutaTMMouse. *Mutagenesis*, 13:601–605.
27. Stuart, GR. *et al.* (2000) Interpretation of mutational spectra from different genes: analyses of PhIP-induced mutational specificity in the lacI and cII transgenes from colon of Big Blue® rats. *Mutat. Res.*, 452, 101–121.
28. Yadollahi-Farsani, M. *et al.* (1996) ACCELERATED PAPER: mutational spectra of the dietary carcinogen 2-amino-1-methyl-6-phenylimidazo[4,5- b]pyridine (PhIP) at the Chinese hamster hprt locus. *Carcinogenesis*, 17, 617–624.
29. Magoč, T. *et al.* (2011) FLASH: fast length adjustment of short reads to improve genome assemblies. *Bioinformatics*, 27, 2957–2963.
30. Carothers, A.M. *et al.* (1994) Mutation and repair induced by the carcinogen 2-(hydroxyamino)-1-methyl-6-phenylimidazo[4,5-b] pyridine (N-OH-PhIP) in the dihydrofolate reductase gene of Chinese hamster ovary cells and conformational modeling of the dG-C8-PhIP adduct in DNA. *Chem. Res. Toxicol.*, 7, 209–218.
31. Ollikainen, M. *et al.* (2007) Mechanisms of inactivation of MLH1 in hereditary nonpolyposis colorectal carcinoma: a novel approach. *Oncogene*, 26, 4541–4549.
32. Zhang, J. *et al.* (2006) Gene conversion is a frequent mechanism of inactivation of the wild-type allele in cancers from MLH1/MSH2 deletion carriers. *Cancer Res.*, 66, 659–664.
33. Lu, S.L. *et al.* (1996) Loss or somatic mutations of hMSH2 occur in hereditary nonpolyposis colorectal cancers with hMSH2 germline mutations. *Jpn. J. Cancer Res.,* 87, 279–287.
34. Shia, J. (2008) Immunohistochemistry versus microsatellite instability testing for screening colorectal cancer patients at risk for hereditary nonpolyposis colorectal cancer syndrome. Part I. The utility of immunohistochemistry. *J. Mol. Diagn.*, 10, 293–300.
35. Bartkova, J. *et al.* (2005) DNA damage response as a candidate anti-cancer barrier in early human tumorigenesis. *Nature*, 434, 864–870.
36. Jiricny, J. (2006) The multifaceted mismatch-repair system. *Nat. Rev. Mol. Cell Biol.*, 7, 335–346.
37. Pilzecker, B. *et al.* (2019) DNA damage tolerance in stem cells, ageing, mutagenesis, disease and cancer therapy. *Nucleic Acids Res.*, 47, 7163–7181.
38. Lv, L. *et al.* (2013) Mismatch repair protein MSH2 regulates translesion DNA synthesis following exposure of cells to UV radiation. *Nucleic Acids Res.*, 41, 10312–10322.